Research, Society and Development, v. 10, n. 2, e48610212328, 2021
(CC BY 4.0) | ISSN 2525-3409 | DOI: http://dx.doi.org/10.33448/rsd-v10i2.12328

Performance Evaluation of the $SrZr_xSn_{1-x}O_3$ Photocatalytic System for Remazol Yellow Dye Degradation Employing Box-Behnken Design

Avaliação de Desempenho do Sistema Fotocatalítico $SrZr_XSn_{1-X}O_3$ para Degradação de Corante Amarelo de Remazol Utilizando o Modelo Box-Behnken

Evaluación del Sistema Fotocatalítico $SrZr_XSn_{1-X}O_3$ Utilizado para la Degradación del Colorante Aamrillo Remazol Empleando Diseño Box-Behnken

Received: 01/25/2021 | Reviewed: 02/14/2021 | Accept: 02/16/2021 | Published: 02/25/2021

Yohanna Ribeiro Kafkle
ORCID: https://orcid.org/0000-0001-7835-2100
Universidade Estadual da Paraíba, Brazil
E-mail: yohannaklafke@gmail.com
Mayara Macedo da Mata
ORCID: https://orcid.org/0000-0001-6364-7475
Universidade Estadual da Paraíba, Brazil
E-mail: mayara.mata@aluno.uepb.edu.br
Ieda Maria Garcia dos Santos
ORCID: https://orcid.org/0000-0002-3349-3994
Universidade Federal da Paraíba, Brazil
E-mail: ieda@quimica.ufpb.br
Mary Cristina Ferreira Alves
ORCID: https://orcid.org/0000-0002-8079-8336
Universidade Estadual da Paraíba, Brazil
E-mail: mary.alves@cct.uepb.edu.br
Simone da Silva Simões
ORCID: https://orcid.org/0000-0002-1863-2933
Universidade Estadual da Paraíba, Brazil
E-mail: simonesimoes@servidor.uepb.edu.br

Abstract
Contamination of effluents often occurs due to improper disposal of textile dyes or their by-products. These can often be carcinogenic and/or mutagenic to the biome. Given the above, the need for effective methods for treating effluents is clear. This treatment occurs by biological, physical, and/or chemical processes. Regarding chemical processes, heterogeneous photocatalysis stands out, mainly because it guarantees an effective degradation of contaminants. In this sense, mixed metal oxides, act as photocatalysts and constitute structures capable of producing a large family of solids with physical properties suitable for the degradation of many pollutants. Modified ABO_3 perovskites, as in the case of the $SrZr_xSn_{1-x}O_3$ semiconductor system, are effective in the degradation of textile dyes in effluents. The present work aimed to use the Box-Behnken model to evaluate the performance of the oxides resulting from the structural modifications of the perovskite $SrZr_xSn_{1-x}O_3$ system, concerning the discoloration of the golden yellow dye remazol. The synthesized oxides were characterized by instrumental techniques and a Box-Behnken 3^4 project was developed. From this, the influence of some factors such as structural modification, oxide mass, exposure time, and the number of UVC lamps was evaluated. The discoloration of the dye was monitored from the attenuation of the absorbance at the wavelength 411 nm. According to the results obtained, the highest percentage of discoloration was obtained using the modified oxide $SrZr_{0,25}Sn_{0,75}O_3$ for an approximate time of 6 hours in contact with 1 UVC lamp.
Keywords: Experimental design; Perovskite, Photocatalysis.

Resumo
A contaminação de efluentes muitas vezes ocorre pelo descarte inadequado de corantes têxteis ou seus subprodutos. Estes muitas vezes podem ser cancerígenos e / ou mutagênicos para o bioma. Diante do exposto fica clara a necessidade de métodos eficazes para o tratamento de efluentes. Este tratamento ocorrer por processos biológicos, físicos e/ou químicos. No tocante aos processos químicos, a fotocatálise heterogênea se destaca, principalmente porque garante uma degradação efetiva dos contaminantes. Neste sentido os óxidos metálicos mistos, atuam como fotocatalisadores e constituem estruturas capazes de produzir uma grande família de sólidos com propriedades físicas adequadas para a degradação de muitos poluentes. As perovskitas do tipo ABO_3 modificadas, como é o caso do sistema semicondutor $SrZr_xSn_{1-x}O_3$, são eficazes na degradação de corantes têxteis em efluentes. O presente trabalho

teve como objetivo utilizar o modelo Box-Behnken para avaliar o desempenho dos óxidos resultantes das modificações estruturais do sistema perovskita $SrZr_xSn_{1-x}O_3$, em relação à descoloração do corante amarelo dourado remazol. Os óxidos sintetizados foram caracterizados por técnicas instrumentais e um projeto Box-Behnken 3^4 foi desenvolvido. A partir deste a influência de alguns fatores como modificação estrutural, massa de óxido, tempo de exposição e o número de lâmpadas UVC foram avaliados. A descoloração do corante monitorada a partir da à atenuação da absorbância no comprimento de onda 411 nm. De acordo com os resultados obtidos o maior percentual de descoloração foi obtido utilizando o óxido modificado $SrZr_{0.25}Sn_{0.75}O_3$ por um tempo aproximado 6 horas em contato com 1 lâmpada UVC.
Palavras-chave: Desenho experimental; Perovskita, Fotocatálise.

Resumen
La contaminación de los efluentes ocurre a menudo debido a la eliminación inadecuada de tintes textiles o sus subproductos. A menudo, estos pueden ser cancerígenos y / o mutagénicos. Dado lo anterior, es clara la necesidad de métodos efectivos para el tratamiento de efluentes. Este tratamiento ocurre por procesos biológicos, físicos y / o químicos. En cuanto a los procesos químicos, destaca la fotocatálisis heterogénea, principalmente porque garantiza una degradación eficaz de los contaminantes. En este sentido, los óxidos metálicos mixtos, actúan como fotocatalizadores y constituyen estructuras capaces de producir una gran familia de sólidos con propiedades físicas aptas para la degradación de contaminantes. Las perovskitas como en el caso del sistema semiconductor $SrZr_xSn_{1-x}O_3$, son eficaces en la degradación de los tintes textiles en los efluentes. El presente trabajo tuvo como objetivo utilizar el modelo de Box-Behnken para evaluar el comportamiento de los óxidos resultantes de las modificaciones estructurales del sistema $SrZr_xSn_{1-x}O_3$, en relación con la decoloración del tinte amarillo dorado remazol. Los óxidos sintetizados se caracterizaron mediante técnicas instrumentales y se desarrolló un proyecto Box-Behnken 3^4. A partir de esto, se evaluó la influencia de factores como la modificación estructural, la masa de óxido, el tiempo de exposición y el número de lámparas UVC. La decoloración del tinte se controló a partir de la atenuación de la absorbancia a la 411 nm. Según los resultados, el mayor porcentaje de decoloración se obtuvo utilizando el óxido $SrZr_{0.25}Sn_{0.75}O_3$ durante un tiempo aproximado de 6 horas en contacto con 1 lámpara UVC.
Palabras clave: Diseño experimental; Perovskita, Fotocatálisis.

1. Introduction

Population growth has caused an increasing demand for consumer goods resulting in expanded industrial development of the textile sector. With the industrial advance the dyes used for dyeing have become synthetic and potentially harmful to the environment. The contamination of effluents during the dyeing process has become a serious problem. The textile industry generates large volumes of contaminated effluent daily, which if not treated and disposed of correctly can cause serious environmental problems (Catanho, Malpass, Motheo, 2006, Soutsas, et al. 2010). For this reason, the removal of these contaminants has become a serious object of study (Mahmouda, et al. 2017, Sainia, et al. 2017, Fabbricino, Pontoni, 2016). In the literature, there are reports on works involving the degradation of this type of contaminant by biological (Correa, et al. 2009), physical (Filtration, coagulation / flocculation), chemical (chemical precipitation, chemical oxidation, adsorption) (Kuns, et al.2002, Dotto, et al. 2011, Vasques, et al. 2011) and photocatalytic processes (Catanho, Malpass, Motheo, 2006, Ramo, et al 2020). Among the chemical processes, Advanced Oxidative Processes (AOPs) have been studied and widely used to ensure an effective degradation of the contaminants (Maeda, Eguchi, Oshima, 2014, Wang, Tadé, Shao, 2015). These AOPs generate hydroxyl radicals that consist of a powerful oxidizing agent. Since the hydroxyl radicals generated are highly reactive and not selective, they can act on the chemical oxidation of a wide range of substances (Peralta-Zamora, et al., 1999, Malato, et al. 2002).

Among the most commonly used AOPs is heterogeneous photocatalysis based on the activation of a semiconductor (catalyst) by sunlight or artificial light. The most applied catalysts are: TiO_2, ZnO, FeO_3, SiO_2, ZnS, all presenting promising results in the degradation of dye in water (Costa, et al. 2004, Cervantes, Zaia, Santana, 2009). The metal oxides of the general formula ABO_3, also called perovskite (Toniolo, et al., 2012), such as $SrSnO_3$ and $CaSnO_3$, act as photocatalysts (Barros Neto, Scarminio, Bruns, 2010). These compounds have versatile structures capable of originating a large family of solids. They were initially studied because they have excellent physical properties such as ferroelectricity, piezoelectricity, pyroelectricity and magnetic effects (Toniolo, et al., 2012). Modified ABO_3-type perovskites, such as the $SrZr_xSn_{1-x}O_3$ semiconductor system,

have shown good results for the degradation of textile dyes in effluents, indicating their suitability in the treatment of industrial effluents. In order to evaluate the degradability of these perovskites, however, it is necessary some experimental parameters must be identified, such as structural modification, quantity of oxide to be used, exposure to UVC light and time of contact of the oxide with the dye.

To evaluate the influence of these parameters, we carried out photocatalytic tests using experimental designs, which are statistical tools that enable the determination of the influence of independent variables and their multivariate and simultaneous interactions (Barros Neto, Scarminio, Bruns, 2010). Indeed, the use of chemometric tolls help to optimize and undertand the catalytical processes and other important processes related to solid materials (Yücela, Yücelb, Durakb, 2016, Meinratha, 1998, Meinratha, Lisd, Elbanowskid, 2004)**.**

2. Methodology

The methodology for the development of this work is structuralist since from the study of the photocatalytic process of removing the yellow dye from remazol and the evaluation of the influence of some experimental parameters, a statistical model was built capable of predicting the percentage of degradation of the dye ahead variations in these experimental parameters.

2.1 Synthesis and characterization of the $SrZr_xSn_{1-x}O_3$

Oxides in the $SrZr_xSn_{1-x}O_3$ modified system (x = 0.25, 0.50 and 0.75) were synthesized based on the Pechini method (Pechini**,** 1967). The method consists of forming a chelate between the metal cations and a carboxylic acid, such as citric acid. The chelate produced was polymerized using ethylene glycol to form a polyester (polymer chain) that was subsequently thermally treated to obtain the crystalline material. Tin and Zirconia citrates were obtained as described in the literature (Cavalcante, et al., 2007, Alves, et al., 2009).

2.1.1 X-ray diffraction

Samples were analyzed using an XRD-6000 X-ray diffraction spectrometer from SHIMADZU, with a power of 2 kVA, a voltage of 30 kV and a current of 30 mA. The slits used were: 1 ° divergence, 1 ° dispersion and 0.3 mm reception slit, with sweeps in the range of 2θ = 10-90 °.

2.1.2 Raman spectroscopy

Measurements were performed using a Raman spectrophotometer with a photoluminescence accessory, coupled to a Renishaw Raman microscope equipped with a solid state laser diode operating at an exposure time of 5 minutes.

2.1.3 UV-visible spectroscopy

Absorption spectra in the UV-Visible region, solid oxide and solutions, were recorded in the 900 to 190 nm region using a spectrophotometer, SHIMADZU, model UV-2550. Solid oxide spectra were used to calculate the gap energy according to the TAUC method (Wood, Tauc, 1972). And the spectra of the solutions were used to evaluate the attenuation of the radiation absorption in the 411nm wavelength.

2.2 Photocatalytic Tests Using Experimental Designs

To evaluate the photocatalytic performance of the oxides resulting from the structural modifications of the $SrZr_xSn_{1-x}O_3$ perovskite system, experimental conditions such as structural modification, amount of oxide to be used, time of exposure and intensity of UV radiation (number of lamps) were identified with the aid of techniques of planning and optimization of experiments. To evaluate the significance of the 4 factors studied, as well as the interactions among them, a Box-Behnken design was used, according to Table1.

Table 1: Factors analyzed and their variations on three levels.

	Level		
Factor	Minimum (-1)	Intermediate (0)	Maximum (+1)
X1	$SrZr_{0.25}Sn_{0.75}O_3$	$SrZr_{0.50}Sn_{0.50}O_3$	$SrZr_{0.75}Sn_{0.25}O_3$
X2	0.0500	0.1000	0.2500
X3	3	6	9
X4	1	2	3

X1: Modification of the oxide; X2: Oxide mass (grams); X3: Exposure Time (hour); X4: Intensity of UV radiation (Nº. of lamps). Source: Authors,

For the accomplishment of the 27 experiments defined by the Box Behnken model, the concentration of the textile dye in water was set at $5mg.L^{-1}$. Each experiment was performed in triplicate. The dye used was remazol golden yellow RNL.

Each experimental system defined by the Box-Benhken model was represented by a beaker 100 mL of the solution containing the dye and the appropriate mass of the oxide (defined by the experimental design). Then, each beaker was placed inside a photocatalytic reactor to expose it to the appropriate amount of UV radiation for the time indicated experimental design. The intensity of the UV radiation was varied according to the number of 30W UV Phillips UVC (254 nm) lamps placed inside the photocatalytic reactor. The dependent variable was the attenuation of the absorbance at the characteristic wavelength of the chromophore responsible for the dye color used (411 nm), related to photocatalytic discoloration of the dye (Ajmal, 2016). This variable was monitored by recording spectra in the UV-vis region.

The experimental design as well as the statistical treatment and evaluation of the data obtained were performed using software Statistica®, Statsoft, version 10.

3. Results and Discussion

3.1 Characterization of the Oxid

3.1.1 X-ray difraction

Figure 1 shows the XRD patterns of the $SrZr_xSn_{1-x}O_3$ system calcined at 700 ° C for 2h under air. We observed well-defined peaks at 700 ° C related to the orthorhombic perovskite structure, according to crystallographic sheets JCPDS 00-044-0161 ($ZrSnO_3$) and 01-077-1798 ($SrSnO_3$) for pure and substituted samples. We can also observe low intensity peaks related to strontium carbonate (#), around 25,3 °; 36.2 °; 44.2 ° and 50.0 °; According to the JCPDS form (01-077-198).

We observed a widening of the peaks and displacement to higher values of θ as a function of the increase of the Zr^{4+} concentration in the $SrZr_xSn_{1-x}O_3$ system. This behavior may be related to the rearrangement of the cation substitution at the octahedron site of the crystalline system, generating greater long-range disorder (Tarrida, Larguem, Madon, 2009).

Figure 1: DRX spectra of $SrZr_xSn_{1-x}O_3$ system patterns calcined at 700 ° C for 2 hours.

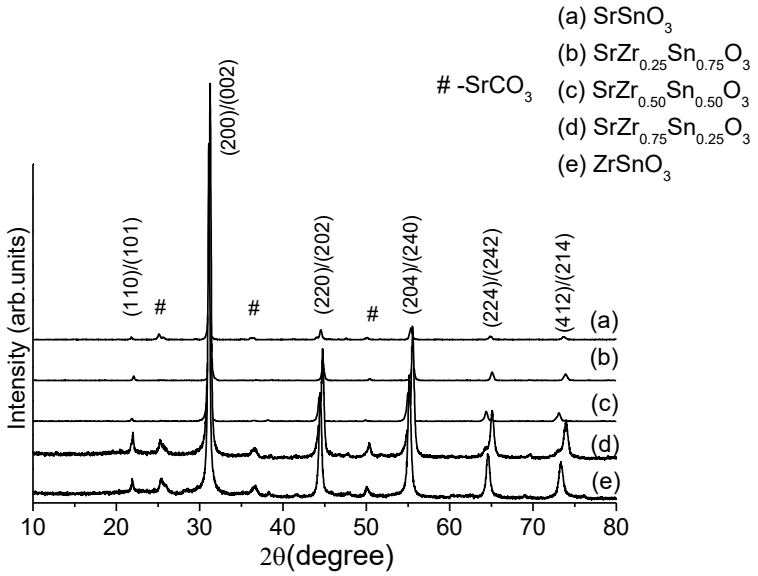

Source: Authors,

3.1.2 Raman spectroscopy

Figure 2 shows the Raman spectra of the $SrZr_xSn_{1-x}O_3$ substituted system. A change of the profile in the region between 147 and 180 cm^{-1}, also known as the lattice modifier region, can be observed in relation to the lattice vibrational modes (dodecahedron site, cation A of ABO_3 structure) (Tarrida, Larguem, Madon, 2009, Zhang, Tang, Ye, 2006).

Figure 2: Raman spectra of the $SrZr_xSn_{1-x}O_3$ modified system: (A) $SrSnO_3$; (B) $SrZr_{0.25}Sn_{0.75}O_3$; (C) $SrZr_{0.50}Sn_{0.50}O_3$; (D) $SrZr_{0.75}Sn_{0.25}O_3$ and (E) $SrZrO_3$.

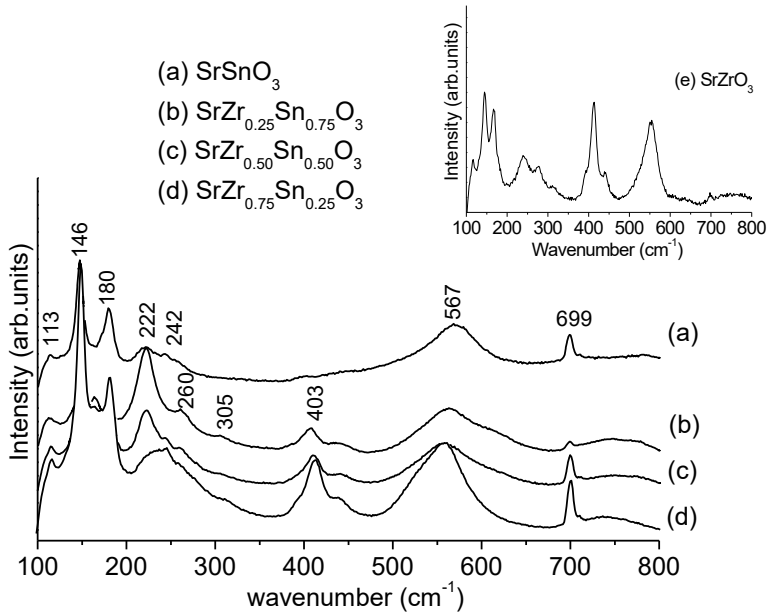

Source: Authors,

The substitution of Sn^{4+} (lower cation) by Zr^{4+} (higher cation) in the $SrZr_xSn_{1-x}O_3$ system promotes significant changes in relation to the active modes in the Raman spectrum of these samples, especially in relation to the sample $SrZr_{0.25}Sn_{0.75}O_3$ (See Figure 2B). This indicates significant changes relative to the region of the lattice former (octahedron site,

cation B of the ABO_3 structure), mainly in relation to the 223 cm^1 region (binding mode, BO), thus presenting a greater number of active modes in the Raman spectrum (See Table 2).

Table 2: Frequencies (cm^{-1}) of the Raman absorption bands and designations for the $SrZr_xSn_{1-x}O_3$ system.

Mode	Obtained in this work					Observed in the literature	
	Sr100%	**Zr25%**	**Zr50%**	**Zr75%**	**Zr100%**	**$SrZrO_3$[1]**	**$SrSnO_3$ [2]**
Lattice (Sr-BO_3)	113(vw)* 147(vs)* 180(s)*	113(vw)* 146(m)* 162 (m)* 180(vw)*	114(w)* 148 (s)* 167(vw)* 180(m)*	116(vw)* 148(vs)* 164(vw)* 181(w)*	116(w)* - - 143(vs)* 163(s)*	95 109 118 134 146 169 193	119 150 168
Bond (B-O)	222(m)* 242(w)*	223(vs)* 262(vw)* 305(vw)*	222(m)* 244(vw)* 261(vw)*	235(w)*	242(m)* 276(w)*	239 279	220 257 305
Torsional (B-O_3)	403(vw)*	405(m)* 436(w)*	409 (m)* 440 (vw)*	309(vw)* 412(m)* 438(vw)*	313(w)* 414(vs)* 440(w)*	316 395 415 442	403
Stretching (B-O)	567(s)*	562(s)*	558(m)*	557(m)*	553(vs)*	478 554	511 596
2nd order vibration (Overlap)	699(m)*	700(w)* 750(m)*	700(m)*	704(m)*	698(w)*	621 655 755	713 890
Total of active modes	**08**	**12**	**11**	**10**	**10**	**18**	**11**

Source: Authors,

As can be observed in Figure 2 and Table 2, there are variations in the profiles of the bands in relation to the region between 407 and 412 cm^{-1} (torsional mode, B-O_3) and 558 to 560 cm^{-1} (stretch mode, BO) for all samples. In addition, we can observe the presence of bands in the region of 698-750 cm^{-1} (Figure 2), which according to the literature are related to second-order vibrations, resulting from overlays of several active modes (Tarrida, Larguem, Madon, 2009, Zhang, Tang, Ye, 2006, Nakamoto, 1986). The behavior of the Raman spectra of the samples in the analyzed $SrZr_xSn_{1-x}O_3$ system, showed that the composition $SrZr_{0.25}Sn_{0.75}O_3$ is able to have a better potential for photodegradation of the dye in relation to the other compositions, because it has a greater number of bands in the Raman spectra. According to the literature, the greater the number of bands observed in the Raman spectra, the greater the degree of distortion of the orthorhombic perovskite structure, the greater polarization of the molecule and consequently the greater migration of electrons in the crystalline lattice (Zhang, Tang, Ye, 2006, Nakamoto, 1986).

3.1.3 UV-Vis spectroscopy

An increase in the amount of the substituent cation Zr^{4+} in the $SrZr_xSn_{1-x}O_3$ system (Table 2) promotes the increase of band gap energy values of the substituted materials, corroborating the behavior observed in the Raman spectra of these materials (See Figure 2), where the composition $SrZr_{0.25}Sn_{0.75}O_3$ presents a greater degree of asymmetry due to the presence of a greater number of active modes in the Raman spectrum (Tarrida, Larguem, Madon, 2009, Zhang, Tang, Ye, 2006, Udawatte, Kakihana, Yoshimura, 2000) in relation to the other substituted samples . Simultaneous competition between the different B

cations at the octahedron sites promotes different levels of electron polarization in the orthorhombic perovskite structure (Zhang, Tang, Ye, 2006, Mountstevens, Attfield, Redfern,2003), which is clear from the different profiles and band numbers presented in the Raman spectra (Figure 2), as well as band gap values obtained from the absorption curves in the visible region of these materials (see Figure 3 and Table 3).

Figure 3: UV-visivel spectra of absortion for $SrZr_xSn_{1-x}O_3$ system.

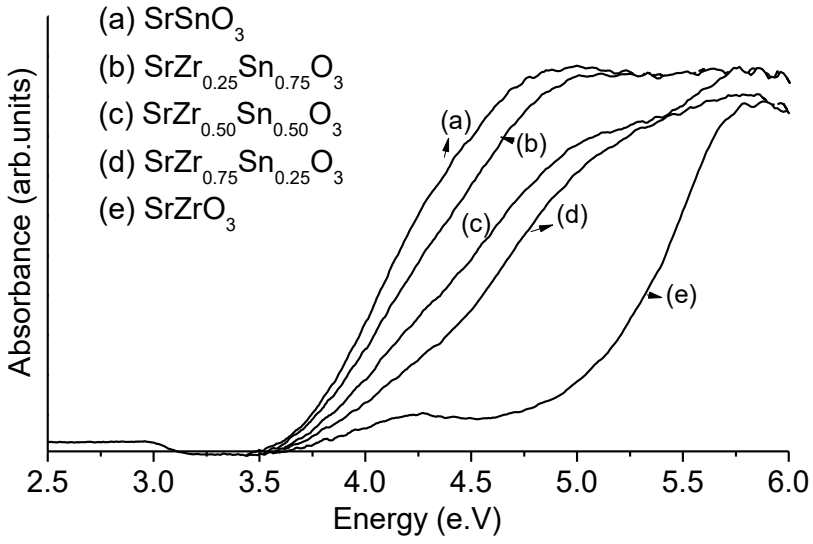

Source: Authors,

Table 3: Band gap values calculated from the absorption spectra of the $SrZr_xSn_{1-x}O_3$ system by the Wood and Tauc method (Wood, Tauc, 1972).

Zr^{4+} concentration in the $SrZr_xSn_{1-x}O_3$ system	**Exp. Gap energy (eV)**
0	3.9
0.25	4.0
0.50	4.2
0.75	4.4
1	5.2

Source: Authors,

3.2 Absorption spectra in the UV-vis of the remazol golden yellow dye

The color of an azo dye, such as Remazol, is a result of the interaction between an azo group (-N = N-) and an aromatic species (Sauer et al., 2005, ZIlle, Gornacka, Rehorek, 2005) The UV-vis absorption spectra of the remazol golden yellow dye at the 5 ppm concentration is shown in Figure 4, where the absorption band of the azo compound (411 nm) and the aromatic ring (238 and 293 nm) can be observed. The efficiency of the decolorizing capacity of the oxide studied was related to absorbance attenuation at wavelength 411 nm.

Figure 4: UV-vis spectra of the remazol golden yellow dye at the concentration of 5 ppm.

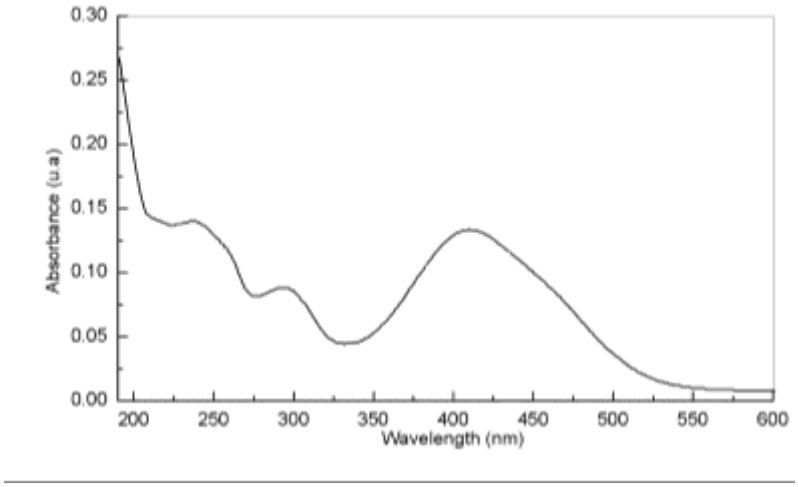

Source: Authors,

3.3 Box-Behnken design

To evaluate of the performance of the synthesized oxides as to the decolorization capacity of the remazol golden yellow dye, a Box-Behnken model was used owing to its ability to evaluate factors at three levels using few experiments. The Box-Behnken model was used to evaluate the performance of the synthesized oxides in relation to their ability to discolor the dye.

3.3.1 Box Behnken statistical analysis

The Box Benkhen design was composed of 27 experiments, carried out in triplicate, in which the factors studied were the relative modification in the stoichiometric of perovskite (in relation to the amount of Zirconium and Tin); mass of oxide added to the dye solution; intensity of the UVC radiation (number of lamps contained in the reactor) and the time of exposure of the dye containing solutions to UVC radiation inside the reactor. The factors were varied at a minimum, intermediate and maximum level. The analyzed response was the absorbance at the wavelength 411 nm, represented by the average of the triplicates.

Initially, a simple model was developed where interactions were not included, i.e., only the main factors were considered. The coefficient of determination (R^2) for this model was 0.75085 and the adjusted R^2 was 0.6401, indicating that 24.91% of the total variation was not explained by the model. The value of adjusted R^2 less than R^2 is related to the small sample size and the amount of terms in the model (Yetilmezsoy, Demirel, Vanderbei, 2009). We tested the model that took into account the linear and quadratic interactions between the factors, except for the quadratic effect of the oxide composition, because this is a stoichiometric ratio. In this case the model had a $R^2 = 1.0000$ and an adjusted $R^2 = 0.9999$. The high value of R^2 demonstrates the high significance of the model and the correlation between the dependent and the independent variables.

The significance of the independent variables and their interactions were tested using ANOVA (Table 4) at a significance level of 0.05 (p=0.05).

Table 4: Analysis of variance for the Box-Behnken model 3^4.

Factor	Squared Sum (SS)	Squared Mean (SM)	F-value	p-value
Structural Change (1)	0.000327	0.000327	98.102,1	0.000010
Mass L+Q (2)	0.000233	0.000116	34.942,2	0.000029
Time L+Q (4)	0.006559	0.003279	983.791,5	0.000001
Lamp L+Q (3)	0.000567	0.000284	85.090,8	0.000012
1 * 2	0.001511	0.000378	113.327,7	0.000009
1 * 3	0.001820	0.000455	136.484,9	0.000007
1 * 4	0.000290	0.000097	28.984,0	0.000035
2 * 3	0.000591	0.000197	59.078,2	0.000017
2 * 4	0.000424	0.000212	63.619,1	0.000016
3 * 4	0.000531	0.000531	159.390,7	0.000006
Error	0.000000	0.000000	-	-
Total SS	0.014541			

Source: Authors,

The standardized effects of the independent variables and their interactions on the dependent variables were analyzed using a Pareto chart. According to the Pareto chart, only the interaction among the quadratic factor oxide modification (X1) vs linear factor oxide mass (X2) are not significant. Regarding the individual factors, the quadratic factor time of exposure were the most significant. These variables were related negatively to the dependent variable; that is, when a longer time was used, there was a lessening in absorbance intensity in the length of the wave under analysis. Intensity of the UVC radiation and oxido mass factors, both linear and quadratic, are positively related to the dependent variable. This same behavior is observed for the composition of the oxide, being in accordance with what we observed in our experiment. That is, the smaller the structural change the greater the degradation capacity of the oxide. The interaction of two linear factors of exposure (X3) versus intensity of UV radiation (X4) and the interaction of two quadratic factors modification of the oxide (X1) versus oxide mass (X2) were the most significant.

The model described by the equation of the second order in the coded form was established, according to the work published by Can, Kaya and Algur (2006), to explain the efficiency of the degradation of the oxide.

$$Y = 0.0204 - 0.0180X_1 + 0.0024X_2 + 0.0067X_2^2 - 0.0705X_3 - 0.0177X_3^2 + 0.0032X_4 + 0.0105X_4^2 - 0.0063X_1X_2 + 0.0098X_1X_2^2 - 0.0003X_1^2X_2 - 0.0129X_1^2X_2^2 + 0.0273X_1X_3 + 0.0104X_1X_3^2 + 0.0206X_1^2X_3 - 0.0009X_1X_3^2 - 0.0031X_1X_4 - 0.0075X_1^2X_4 - 0.0046X_1^2X_4^2 + 0.0051X_2X_3 + 0.0018X_2X_3^2 + 0.0167X_2^2X_3 + 0.0008X_2X_4 - 0.0145X_2^2X_4 + 0.0230X_3X_4$$

According to the F values of the ANOVA table (Table 4) the Fcalc> Ftabelado (1,26) = 4.23 demonstrating that the model is significant.

Response surface graphs (RS), where two factors are varied while the other factors remain fixed, are useful to understand the behavior of the individual factors as well as their interactions. The RS graph shown in Figure 5 illustrates the effect of the interaction between exposure time and oxide composition on absorbance attenuation at wavelength 411 nm.

Figure 5: Response surface graph to the interaction between oxide composition and time of exposition.

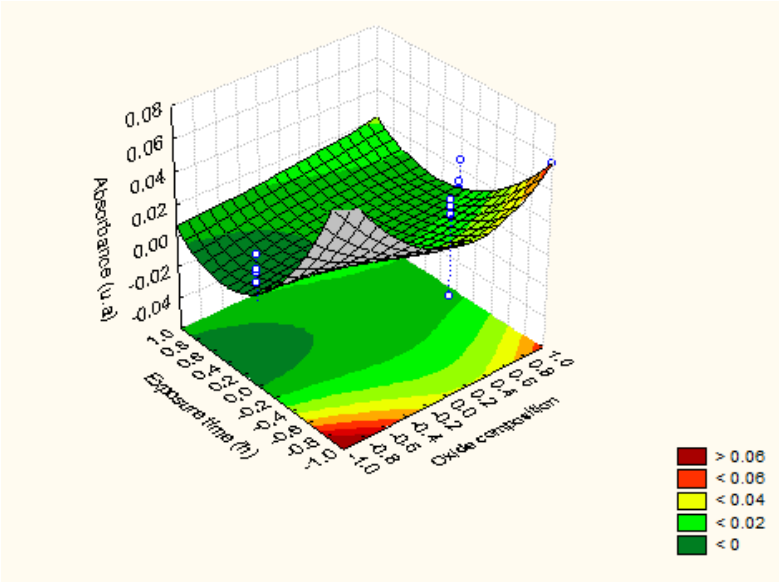

It may be noted that lower absorbance values are obtained when an oxide with minimal ($SrZr_{0.25}Sn_{0.75}O_3$) structural modification is used and it is exposed for more than 6 hours to the UVC radiation. However, after approximately 5 hours the chart shows a decrease in the absorbance values, which indicates that the discoloration was already occurring. The mass and the intensity of UVC radiation *are* at the intermediate level.

The RS graph in Figure 6 shows the relationship between time and UVC radiation intensity.

Figure 6: Response surface graph shows the relationship between time and intensity of the UVC lamp radiation.

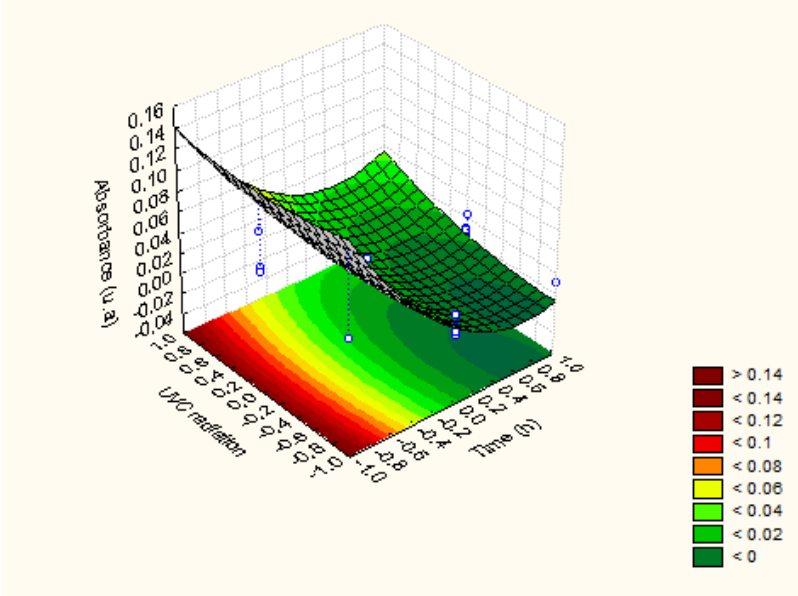

According to this graph the lowest absorbance values are reached at times longer than 6 hours, using one lamp. In this case, the composition was fixed at the intermediate level and mass at the minimum level. The evaluation of the individual experiments confirmed the conclusions obtained through the statistical analysis of the data. The percentage of discoloration for these experiments was approximately 97%, calculated according to the following equation (Weng, Tao, 2015, Sales, et al., 2014).

4. Final Considerations

Perovskite $SrZr_xSn1\text{-}xO_3$ was successfully obtained with the polymer precursor method, based on the Pechini method. These methods were characterized by Raman spectra and X-ray diffraction analysis, which confirmed their crystalline phases by peak indexing using crystallographic data sheets JCPDS 00-044-0161 ($ZrSnO_3$) and 01-077-1798 ($SrSnO_3$).

The photocatalytic performance of the oxides resulting from the structural modifications of the $SrZr_xSn_{1-x}O_3$ type perovskite system relative to the discoloration of remazol golden yellow dye was evaluated using a Box Beckhen experimental design. This permitted a performance evaluation of the oxides resulting from structural modifications. In this experimental design, four independent variables were evaluated: structural modification, amount of oxide used (grams), time of exposure (hours) and intensity of UV radiation (number of lamps). The dependent variable evaluated was the attenuation of the absorbance at the characteristic wavelength (411 nm) of the chromophore responsible color related to photocatalytic discoloration of the dye. The evaluation of the Box-Behnken model showed that the oxides that presented the best discoloration performances were $SrZr_{0.25}Sn_{0.50}O_3$ or $SrZr_{0.50}Sn_{0.50}O_3$, for exposure times longer than 6 hours and using 1 lamp. The model explains the efficiency of the degradation of the oxide.

Thus, according to the data obtained, we can affirm that the application of the modified oxides for the degradation of remazol golden yellow dye is a viable treatment for water reuse and reduces pollution of the water bodies by textile industries. And the Box Behnken planning model is an adequate tool for the evaluation of the photocatalytic capacity of these oxides providing multivariate and scientific interpretation of the action of individual factors and their interactions.

Chemistry, like most sciences, has a great potential to meet the demands of society as well as improve living and health conditions. For the continuation of this research and for it to be effectively applied to society's problems, studies will be carried out on real samples, that is, effluents from the textile industry.

Acknowledgments

The authors thank the agencies CNPq for support and the Laboratory of Fuels and Materials of the Department of Chemistry of the Center of Exact Sciences and Nature of the Federal University of Paraíba, LACOM/DQ/CCEN/ UFPB. And Dystes Ltda, Suzano, São Paulo, Brazil, for the donation of the remazol golden yellow dye.

The English text of this paper was revised by Sidney Pratt, Canadian, MAT (The Johns Hopkins University), RSAdip - TESL (Cambridge University).

References

Ajmal, A., Majeed, I., Malika, R.N., Iqbala, M Nadeemb, M. A., Hussaina, I, & Nadeema, M. A. (2016). Photocatalytic degradation of textile dyes on Cu2O-CuO/TiO2 anatase powders. *Journal of Environmental Chemical Engineering*, 4, 2138–2146.

Alves, M.C F., Souza, S.C., Lima, H, H. S., Nascimento, M. R. M., Silva, R.S., Espinosa, J.W.M., & Santos, M. G. (2009). Synthesis of CaSnO3-SrSnO3 thin films by Chemical Solution Deposition, *J. Alloys Compd* ,476, 507-512.

Barros Neto, B., Scarminio, I. S., & Bruns, R. E. (2010). *Como fazer experimentos.* Campinas Bookman, 4.

Can, M. Y., Kaya, Y., & Algur, O.F. (2006). Response surface optimization of the removal of nickel from aqueous solution by cone biomass of Pinus sylvestris, *Bioresour. Technol*. 97 1761–1765.

Catanho, M., Malpass, G. R. P., & Motheo, A. J. (2006). Avaliação dos tratamentos eletroquímico e fotoeletroquímico na degradação de corantes têxteis, *Quim. Nova*, 29, 983-989.

Cavalcante, L. S., Simões, A. Z, Sczancoski, J. C., Longo, V. M., Erlo, R., & Varela, J. A. (2007). SrZrO3 powders obtained by chemical method: Synthesis, characterization and optical absorption behavior, *Solid State Sciences*, 9, 1020-1027.

Cervantes, T. N. M., Zaia, D. A. M., & Santana, H. (2009). Estudo da fotocatálise heterogênea sobre ti/tio2 na descoloração de corantes sintéticos, *Química Nova*, 32, 2423-2428.

Correa, C. A. R., Aquino S. F., Caldas P. C. P., & Silva S. Q. (2009). Uso de extrato de levedura como fonte de carbono e de mediadores redox, para a degradação anaeróbia de corante azo, *Engenharia Sanitária Ambiental*, 14, 559 – 568.

Costa, F. A. P., Reis, E. M., Azevedo, J. C. R., & NozakI, J. (2004). Bleaching and photodegradation of textile dyes by H2O2 and solar or ultraviolet radiation, *Solar Energy*, 77, 29 – 35.

Dotto, G.L., Vieira, M., L.G., Gonçalves, O. J., L., & Pinto, A. A. (2011). Remoção dos corantes azul brilhante, amarelo crepúsculo e amarelo tartrazina de soluções aquosas utilizando carvão ativado, terra ativada, terra diatomácea, quitina e quitosana: estudos de equilíbrio e termodinâmica. *Quim. Nova*, 34, 1193-1199.

Fabbricino, M., & Pontoni L. (2016). Use of non-treated shrimp-shells for textile dye removal from wastewater, *Journal of Environmental Chemical Engineering*, 4 Part A, 4100–4106.

Kunz, A., Peralta-Zamora P., Gomes de Moraes S., & Durán N. (2002). Novas tendências no tratamento de efluentes têxteis, *Quim. Nova*, 25, 78-82.
M. P. Pechini, U.S. Patent 3.330.697 (1967).

Maeda, K., Eguchi, M., & Oshima, T. (2014). Perovskite Oxide Nanosheets with Tunable Band-Edge Potentials and High Photocatalytic Hydrogen-Evolution Activity, *Ang Chem Internat*, 53, 13164–13168.

Mahmouda, M. S., Mostafab M. K., Mohamedc S. A., Sobhya N. A., & Nasrd M. (2017). Bioremediation of red azo dye from aqueous solutions by Aspergillus niger strain isolated from textile wastewater, *Journal of Environmental Chemical Engineering*, 5, 547–554.

Malato, S., Blanco, J., Fernandez-alba, A. R., & Aguera, A. (2002). Solar photocatalytic meneralization of commercial pesticides: acrinathrin, *Chemosphere*, 235.

Meinratha, G. (1998). Chemometric analysis: Uranium (VI) hydrolysis by UV-Vis spectroscopy, Journal of Alloys and Compounds, 275, 777–781.

Meinratha, G., L. S., & Elbanowskid, M. (2004). Spectroscopy, chemometrics and metrology—three aspects of lanthanide chemistry, *Journal of Alloys and Compound*s, 380, 413–417.

Mountstevens, E. H., Attfield, J. P. E, & Redfern, S. A. T. (2003). Cation-size control of structural phase transitions in tin perovskitas, *J. Phys*, 15, 8315-8326.

Nakamoto, K. (1986). *Infrared and raman spectra of inorganic and coordination compounds*. John Wiley e Filhos.

Peralta-Zamora, P. K., Moraes, A. S. G., Pelegrini, R., Moleiro, P. C., Reyes, J., Mansilla, H., & Duràn, N. (1999). Degradation of reactive dyes I, A comparative study of ozonation, enzymatic and photochemical processes. *Chemosphere*, 38, 835-852.

Pereira, A. S., Shitsuka, D. M., Parreira, F. J., & Shitsuka, R. *Metodologia da Pesquisa Científica*. (pg 28-29) UFSM.

Ramo, L. B., Silva, A. G., Pereira, C. X., Torres, C. S., Silva Júnior, E. P., Martins, G. C., Torres, M. C. M., Alves M. C. F., & Simões, S. S (2020). Microcystin-LR removal in water using the system $SrZr_XSn_{1-X}O_3$: influence of B cation on the structural organization of perovskite. *Chemical Papers*. https://doi.org/10.1007/s11696-020-01423-8.

Sainia, J., Gargb V. K., Guptaa R. K., & Katariac N. (2017). Removal of Orange G and Rhodamine B dyes from aqueous system using hydrothermally synthesized zinc oxide loaded activated carbon (ZnO-AC), Journal of Environmental Chemical Engineering, 5, 884–892.

Sales, H. B., Bouquet, V., Députier, S., Ollivier, S., Gouttefangeas, F., Guilloux-viry M., & Santos. I. M. G. (2014). Sr1_xBaxSnO3 system applied in the photocatalytic discoloration of an azo-dye, *Solid State Sciences*, 28, 67-73.

Sauer, T. P., Casaril, L., Humeres, E., & Moreira, R. F. P. M. (2005). "Mass transfer and photocatalytic degradation of leather dye using TiO2/UV," *Journal of Applied Electrochemical*, 35. 821–829.

Soutsas, K., Karayannis, V., Poulios, I. A., Ntampegliotis, K., Spiliotis, X., & Papapolymerou, G. (2010). Decolorization and degradation of reactive azo dyes via heterogeneous photocatalytic processes, Desalination, 250, 345–350.

Tarrida, M., Larguem, H., & Madon, M. (2009). Structural investigations of (Ca,Sr)ZrO3 and Ca(Sn,Zr)O3 perovskite compounds, *Phys Chem Miner*, 36, 403–413.

Toniolo, J. F. S., Toniolo, R. N. S. H., Magalhães, C. A. C., & Perez, M. S. (2012). Structural investigation of LaCoO3 and LaCoCuO3 perovskite-type oxides and the effect of Cu on coke deposition in the partial oxidation of methane, *Applied Catalysis. B Environmental*, 117-118, 156-166.

Udawatte, C. P., Kakihana, M., & Yoshimura, M. (2000). Low temperature synthesis of pure SrSnO3 and the (Bax Sr1-x) SnO3 solid solution by the polymerized complex method, *Solid State Ionics*, 128: 217.

Vasques, A. R., Souza, M. A. G. U., L. Weissenberg, L., & Souza, A. A. U. (2011). Adsorção dos corantes RO16, RR2 e RR141 utilizando lodo residual da indústria têxtil, *Eng Sanit Ambient*, 16, 245 – 252.

Wang, W. M. O., Tadé, M. O., & Shao, Z. (2015). Research progress of perovskite materials in photocatalysis- and photovoltaics-related energy conversion and environmental treatment, *Chem. Soc. Ver*., 44, 5371-5408.

Weng, C-H., & Tao, H. (2015). Highly efficient persulfate oxidation process activated with Fe0 aggregate for decolorization of reactive azo dye Remazol Golden Yellow. *Arabian Journal of Chemistry*.

Wood, D. L., Tauc, J., & Weak (1972).Absorption Tails in Amorphous Semiconductors. *Phys*. Rev 5.

Yetilmezsoy, K., Demirel, S., & Vanderbei, R. J. (2009). Response surface modeling of Pb (II) removal from aqueous solution by Pistacia vera L.: Box–Behnken experimental design, *Journal of Hazardous Materials*, 171, 551–562.

Yücela, E., Y., & Yücelb, M. D. (2016). Process optimization for window material CdS thin films grown by a successive ionic layer adsorption and reaction method using response surface methodology, *Journal of Alloys and Compounds*, 664, 530–537.

Zhang, W. F. J., & Tang, J. Ye. (2006). Photoluminescence and photocatalytic properties of SrSnO3 perovskite. *Chem. Phys. Lett*., 418, 174–178.

ZIlle, A. Gornacka, B., Rehorek, A., & Cavaco-paulo, A. (2005). Degradation of Azo Dyes by Trametes villosa Laccase over Long Periods of Oxidative Conditions, Applied and Environmenta*l Microbiology*, 71, 6711-6718.